NANO LETTERS
Cite This: Nano Lett. XXXX, XXX, XXX−XXX
Letter
pubs.acs.org/NanoLett

# Time-Resolved Small-Angle X-ray Scattering Reveals Millisecond Transitions of a DNA Origami Switch

Linda K. Bruetzel,[†] Philipp U. Walker,[†] Thomas Gerling,[‡] Hendrik Dietz,[‡] and Jan Lipfert*[,†]

[†]Department of Physics, Nanosystems Initiative Munich, and Center for Nanoscience, LMU Munich, Amalienstrasse 54, 80799 Munich, Germany

[‡]Physik Department, Institute for Advanced Study, Technische Universität München, Am Coulombwall 4a, 85748 Garching, Germany

Supporting Information

**ABSTRACT:** Self-assembled DNA structures enable creation of specific shapes at the nanometer−micrometer scale with molecular resolution. The construction of functional DNA assemblies will likely require dynamic structures that can undergo controllable conformational changes. DNA devices based on shape complementary stacking interactions have been demonstrated to undergo reversible conformational changes triggered by changes in ionic environment or temperature. An experimentally unexplored aspect is how quickly conformational transitions of large synthetic DNA origami structures can actually occur. Here, we use time-resolved small-angle X-ray scattering to monitor large-scale conformational transitions of a two-state DNA origami switch in free solution. We show that the DNA device switches from its open to its closed conformation upon addition of $MgCl_2$ in milliseconds, which is close to the theoretical diffusive speed limit. In contrast, measurements of the dimerization of DNA origami bricks reveal much slower and concentration-dependent assembly kinetics. DNA brick dimerization occurs on a time scale of minutes to hours suggesting that the kinetics depend on local concentration and molecular alignment.

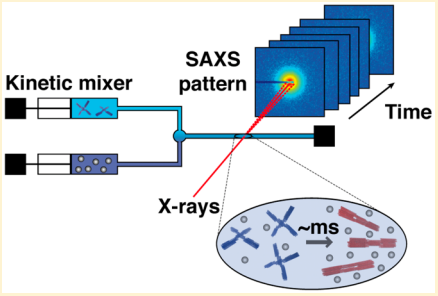


**KEYWORDS:** *DNA nanotechnology, DNA origami, small-angle X-ray scattering, SAXS, time-resolved SAXS, conformational changes*

The programmable self-assembly of DNA molecules is a new paradigm for creating structures at the nanometer−micrometer scale with potential for diagnostic, therapeutic, and engineering applications.[1−4] DNA origami structures are assembled from kilobase long single-stranded (ss) DNA (scaffold) strands that fold due to a number of specific ssDNA oligonucleotides (staple strands) into predefined and precisely addressable approximately megadalton (MDa)-sized structures.[5−7] Recently, further hierarchical organization of DNA origami structures into higher-order assemblies, some of which reaching the approximate gigadalton (GDa) range, has been demonstrated.[8−10] Moving beyond static two- and three-dimensional structures[5,6] toward building complex devices will require implementing and controlling reversible mechanical movements in DNA objects, which remains a challenging aspect in the field.[11] So far, most switchable DNA devices have been triggered by the addition of DNA single strands and toehold-mediated strand exchange, where transitions occur on time scales of minutes. Conformational changes controlled by the addition and exchange of oligonucleotides are fundamentally constrained by the maximal rate of toehold-mediated strand exchange ∼5 × $10^5$ $M^{-1}·s^{-1}$;[12] at typical nanomolar−micromolar concentrations, this corresponds to changes on the time scale of seconds to minutes.[13−16] Conformational transitions initiated by changes in ionic strength, pH, temperature, or light can be faster, and have been demonstrated to occur within seconds.[17,18] A new technology to create well-defined and reversible conformational changes of DNA origami devices relies on shape complementary protrusions and recessions that interact via DNA stacking interactions.[19,20] While salt and temperature-dependent conformational changes of DNA devices based on shape complementary and stacking interactions have been characterized,[19,20] it is an open question how fast conformational transitions of these large, approximately MDa DNA origami structures can be. Friction with the solvent and energy barriers in junctions or pivots could pose fundamental speed limits for switching dynamics, similar to what is observed for folding of naturally occurring RNAs due to their rugged free energy landscapes (Supporting Figure S1).[21,22]

**Fast Conformational Transition of a DNA Origami Switch Device Revealed by trSAXS.** To address this question, we employ time-resolved small-angle X-ray scattering (trSAXS) to monitor conformational transitions in a unimolecular, two-state DNA origami switch and in a bimolecular DNA origami reaction system. SAXS can monitor the conformational transitions of macromolecules and their assemblies in free solution under virtually arbitrary solution conditions.[20,23−27] SAXS does not require any labeling and directly probes the global conformation in solution. By using a

Received: February 9, 2018
Revised: March 19, 2018
Published: March 20, 2018




DOI: 10.1021/acs.nanolett.8b00592
Nano Lett. XXXX, XXX, XXX−XXX

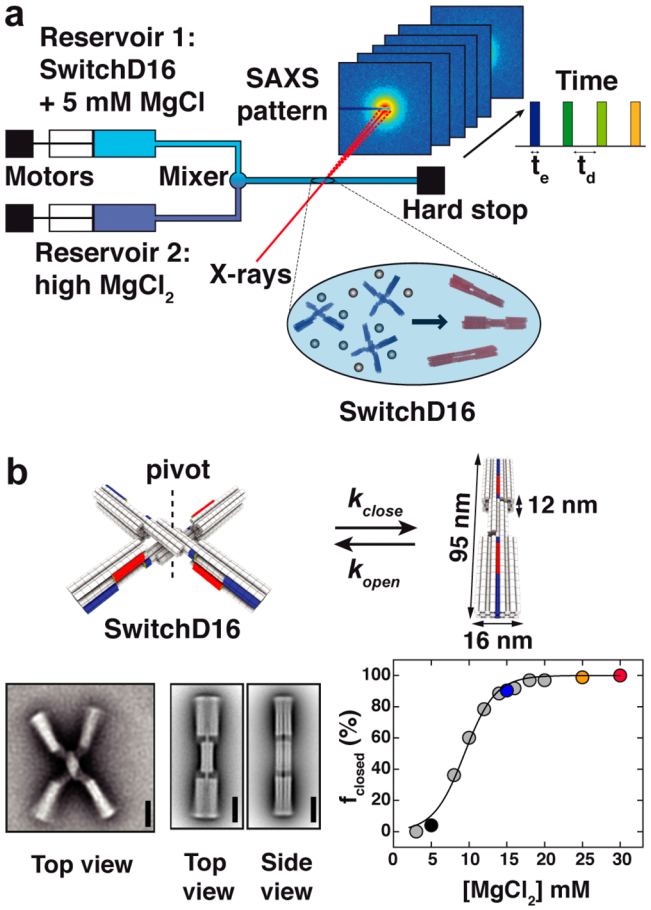


**Figure 1.** Schematic of time-resolved SAXS and a $MgCl_2$-dependent DNA origami switch device. (a) Schematic of the stopped-flow mixing device coupled to the high brilliance beamline ID02 at the ESRF. The mixing reservoirs 1 and 2 contain the switchD16 device in 5 mM $MgCl_2$ and buffer with high $MgCl_2$ concentrations, respectively. After turbulent mixing, the mixture is directed to a capillary and the flow is stopped. The beam hits the sample in a specific acquisition pattern defined by the exposure time ($t_e$) and a delay time ($t_d$) (see Supporting Information). (b) (Top) Schematic view of the switchD16 device, which changes from an open to a closed conformation upon the addition of $MgCl_2$. The closed state is stabilized by 16 basepair stacking interactions occurring at the interface of shape-complementary double helical protrusions (red) and recessions (blue). (Bottom, left) Negative-stain TEM micrographs of switchD16 particles in the presence of 5 mM and 25 mM $MgCl_2$ (scale bars, 20 nm). (Bottom, right) Equilibrium fraction of closed switchD16 devices as a function of $MgCl_2$ determined by SAXS and two-state based thermodynamic model (black line).

stopped-flow kinetic mixer to trigger conformational changes by rapid changes in $MgCl_2$ concentration and a high-flux synchrotron beamline for fast data acquisition,[28] we achieved a time resolution of 25 ms (Figure 1a). We applied trSAXS to study the dynamics of a DNA origami switch (switchD16).[19] We have previously characterized the structure and equilibrium conformations of switchD16.[19,20] In brief, switchD16 consists of two ~100 nm long rigid arms connected by a Holliday junction at the center that allows for reversible transitions between an open and a closed conformation (Figure 1). Shape-complementary patterns of blunt-ended double helical protrusions and recessions are arranged on both arms that can form 16 basepair stacking interactions in the closed conformation of the switch. Electrostatic repulsion counteracts the stacking contacts, such that at low cation concentration the open conformation is favored. We have previously demonstrated that SAXS can monitor and quantify the $MgCl_2$-dependent unimolecular equilibrium of the switchD16 device[20] and determined the midpoint of the open-to-close transition at ~10 mM $MgCl_2$ (Figure 1b and Supporting Information). In the trSAXS measurements, we started with DNA switch devices in 5 mM $MgCl_2$ where the open conformation is predominantly populated (fraction closed $f_{closed}$ < 4%).[20] Using the stopped-flow mixer (see Supporting Information), we then rapidly (within ≤1 ms) added $MgCl_2$ to final concentrations of 15, 25, and 35 mM (where in equilibrium $f_{closed}$ = 90%, 98%, and 99%, respectively) and monitored the subsequent conformational changes. For the 15 mM $MgCl_2$ condition, the transition from the open to the closed state is resolved and well described by a first-order kinetic model (Figure 2 and Supporting Figure S2) with a closing rate constant $k_{close}$ = 22 $s^{-1}$ and an opening rate constant $k_{open}$ = 2.4 $s^{-1}$. For the 25 and 35 mM $MgCl_2$ conditions, the transition to the closed state occurs essentially

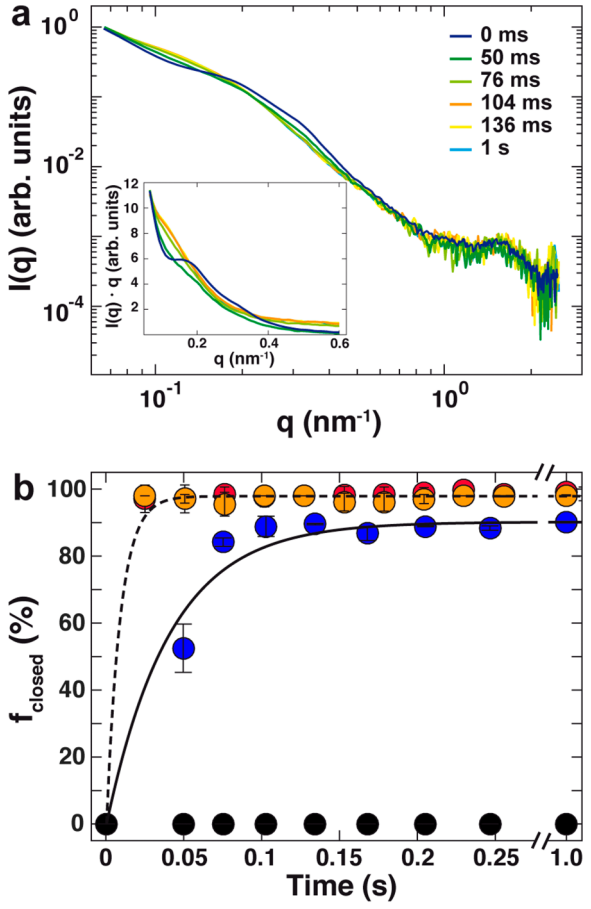


**Figure 2.** TrSAXS reveals conformational kinetics of a DNA origami switch device. (a) SAXS profiles for switchD16 for selected time points after increasing $MgCl_2$ concentration to 15 mM. The inset shows a zoom of the data in Holzer representation ($I(q)\cdot q$ vs $q$). (b) Fraction of switchD16 devices in the closed conformation versus time after changing to $MgCl_2$ concentrations of 5 mM (black circles), 15 mM (blue circles), 25 mM (orange circles), and 35 mM (red circles). Symbols and error bars are the mean and standard deviation from two independent repeats of each condition. The solid black line and dashed black line represent a reversible unimolecular first-order reaction fit to the data at 15 and 25 mM $MgCl_2$ (see Supporting Information).


DOI: 10.1021/acs.nanolett.8b00592
Nano Lett. XXXX, XXX, XXX−XXX

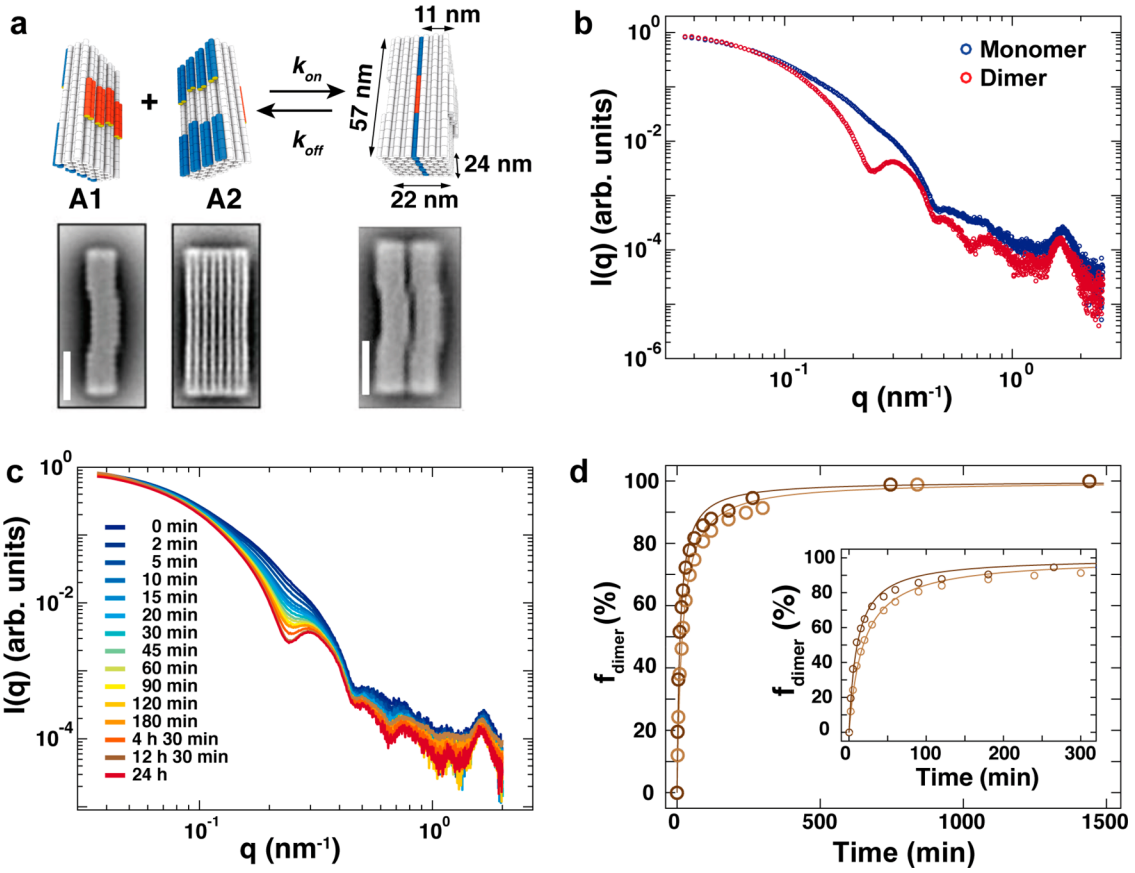


**Figure 3.** Time-resolved SAXS measurements on dimerization kinetics of DNA origami bricks. (a) (Top) Schematic of DNA origami brick monomers with double helical protrusions and recessions (indicated in red and blue) allowing for the formation of a dimeric brick in the presence of 20 mM $MgCl_2$. (Bottom) TEM micrographs of DNA origami monomers and dimers. Scale bar: 20 nm. (b) Experimental scattering profiles of DNA origami monomers (blue circles) and dimers (red circles) at a sample concentration of 100 nM in 20 mM $MgCl_2$. (c) Time evolution of scattering profiles after 1:1 mixing of monomeric brick samples at an initial concentration of 100 nM. (d) Fraction of dimeric brick particles as a function of time determined from a two-state model for initial monomer concentrations of 100 nM (dark brown circles) and 50 nM (light brown circles). Solid lines represent fits of an irreversible bimolecular reaction rate model (see eq 9 Supporting Information) yielding an average association reaction rate constant of $1.7 \times 10^4$ $M^{-1}{\cdot}s^{-1}$. The inset shows a close up of the early time points.

within the dead time of our instrument (25 ms). Analysis of the data suggests a lower limit on the closing rate constants of $k_{close} = 150\ s^{-1}$ (Figure 2b and Supporting Figure S3). The measured closing times of $\tau_{close} = k_{close}^{-1} \leq 7$ ms are at most 1−2 orders of magnitude slower than a simple estimate of the time scale for the diffusive motion of the two arms from the open into the closed state of $\tau_{diff} \sim 100\ \mu s$ (Supporting Text and Supporting Figure S4), suggesting that the DNA switch closes near the diffusive speed limit. Residual energy barriers, if any, for closing must be lower than $\ln(\tau_{close}/\tau_{diff}) \sim 4\ k_BT$, where $k_BT$ is the thermal energy.

**Slow Dimerization of DNA Origami Bricks.** As a reference construct, we studied the kinetics of a bimolecular reaction system consisting of two separate monomeric DNA origami bricks that dimerize via shape-complementary basepair stacking interactions, similar to the switch device (Figure 3a). The SAXS profiles at 20 mM $MgCl_2$ show pronounced differences between the monomer and dimer scattering patterns (Figure 3b). In particular, the scattering profile of the dimeric complex exhibits a clear peak at $q \approx 0.28\ nm^{-1}$ (Figure 3b), which corresponds to a length scale of $2\pi/q \approx 23$ nm that matches the cross-section of the dimer (22 nm × 24 nm) (Figure 3a). This strong interference peak is largely missing in the monomeric profile due to the asymmetric cross sectional area (11 nm × 24 nm) (Figure 3a). On the basis of a two-state model, we determined the fraction of dimers at each time point (Figure 3c,d, Supporting Figure S5, and Supporting Information). As expected for a bimolecular system, we find concentration-dependent assembly kinetics. From a fit of a bimolecular reaction kinetics model to the data we obtain a negligible dissociation rate constant $k_{off}$ and an estimate of an association rate constant $k_{on}$ of $1.7 \times 10^4$ $M^{-1}{\cdot}s^{-1}$. A simple estimate for the time scale of diffusive reaction that takes into account the global dimensions of the bricks yields a diffusion-limited reaction rate constant $k_{diff}$ of $\sim 2.5 \times 10^8$ $M^{-1}{\cdot}s^{-1}$ (see Supporting Information). Hence, the brick system reacts much slower than the diffusive speed limit, which points to the existence of additional barriers, likely to overcome electrostatic repulsion and to achieve the correct alignment of the brick monomers,[29] that slow down the reaction.

Taken together, these data suggest that the very rapid closing transition of the DNA switch device is because the central Holliday junction links the two arms and orients them favorably to form the 16 basepair stacking interactions that stabilize the closed state. Therefore, the central pivot link creates a high effective concentration (estimated to be $k_{close}/k_{on} \sim 1.4$ mM) of the two arms enabling them to interact on the millisecond time scale.



DOI: 10.1021/acs.nanolett.8b00592
Nano Lett. XXXX, XXX, XXX−XXX

In conclusion, we have demonstrated that ~5 MDa DNA origami devices can undergo very fast conformational dynamics on the millisecond time scale, suggesting that such devices could be employed for switching and sensing molecular capabilities with rapid response times. Although the kinetics for the DNA switch device are very fast and approach the estimated diffusion controlled rate, assembly of the DNA bricks at nanomolar−micromolar concentrations is much slower than both the dynamics of the DNA switch, the estimated diffusion controlled rate, and the maximal rate for toehold-mediated strand exchange. In particular, because hierarchical assembly of (various types of) DNA bricks forms the basis for creating higher-order DNA structures reaching the approximate GDa-range,[8,10] it is desirable to better understand and ultimately optimize their assembly kinetics. Unforeseen barriers that could slow down the dimerization dynamics could be caused by deviations of the actual brick geometry from the designed one. For example, residual twist in honeycomb structures[8] may make it necessary that the bricks deform through thermal fluctuations in order to satisfy the stacking bonds. The associated energetic penalties will be likely on the order of multiple $k_BT$ and could thus explain the slow binding rates that we have observed. Thus, one approach for increasing the speed of DNA brick association may consist in more precise design. Other approaches might include optimized temperature and salt conditions, introduction of confinement or molecular crowding agents, chemical modifications to the DNA to reduce charge repulsion, and a more symmetric design to facilitate correct alignment.

Our work establishes trSAXS as a powerful tool to monitor large-scale conformational changes and assembly of DNA origami objects on time scales from milliseconds to hours without the need for labeling or surface immobilization. The ability of SAXS to directly probe the global conformation in solution is advantageous, because it has recently been demonstrated that inferring global conformations from local distance measurements, for example, by Förster resonance energy transfer (FRET), can be problematic[30,31] and that the addition of dyes can bias the conformational ensemble.[32] In the future, a combination of continuous-flow mixing in appropriate microfluidics with microfocus X-ray sources has the potential to push the time-resolution even into the microsecond-regime,[33] which would allow us to directly probe conformational transitions at the molecular speed limit.

## ■ ASSOCIATED CONTENT

### Supporting Information

The Supporting Information is available free of charge on the ACS Publications website at DOI: 10.1021/acs.nanolett.8b00592.

Methods, text, and Figures S1−S8 (PDF)

## ■ AUTHOR INFORMATION


### Corresponding Author

*E-mail: Jan.Lipfert@lmu.de. Phone: +49-89-2180-2005.

### ORCID

Jan Lipfert: 0000-0003-3613-7896


### Author Contributions

L.K.B. and P.U.W. contributed equally to this work. All authors designed this study. T.G. assembled and purified DNA origami samples; L.K.B. and P.U.W. performed SAXS measurements and analyzed the data. All authors contributed to writing the paper and have given approval to the final version of the manuscript.


### Funding

This work was supported by the Deutsche Forschungsgemeinschaft through grants provided within Gottfried-Wilhelm Leibniz Program, the Excellence Clusters CIPSM (Center for Integrated Protein Science Munich), NIM (Nanosystems Initiative Munich), and the Sonderforschungsbereich SFB863.


### Notes

The authors declare no competing financial interest.

## ■ ACKNOWLEDGMENTS


We thank Dr. Theyencheri Narayanan for assistance at beamline ID02 and Dr. Martha Brennich for help at beamline BM29 at the ESRF (Grenoble, France), Dr. Martin Schroer for assistance at beamline P12 at DESY (Hamburg, Germany), Florian Praetorius for scaffold DNA preparations, and Philip Tinnefeld for discussions.


## ■ REFERENCES


(1) Siavashpouri, M.; Wachauf, C. H.; Zakhary, M. J.; Praetorius, F.; Dietz, H.; Dogic, Z. *Nat. Mater.* **2017**, *16*, 849−856.
(2) Halley, P. D.; Lucas, C. R.; McWilliams, E. M.; Webber, M. J.; Patton, R. A.; Kural, C.; Lucas, D. M.; Byrd, J. C.; Castro, C. E. *Small* **2016**, *12*, 308−20.
(3) Schmied, J. J.; Gietl, A.; Holzmeister, P.; Forthmann, C.; Steinhauer, C.; Dammeyer, T.; Tinnefeld, P. *Nat. Methods* **2012**, *9*, 1133−4.
(4) Ponnuswamy, N.; Bastings, M. M. C.; Nathwani, B.; Ryu, J. H.; Chou, L. Y. T.; Vinther, M.; Li, W. A.; Anastassacos, F. M.; Mooney, D. J.; Shih, W. M. *Nat. Commun.* **2017**, *8*, 15654.
(5) Rothemund, P. W. *Nature* **2006**, *440*, 297−302.
(6) Douglas, S. M.; Dietz, H.; Liedl, T.; Hogberg, B.; Graf, F.; Shih, W. M. *Nature* **2009**, *459*, 414−8.
(7) Dietz, H.; Douglas, S. M.; Shih, W. M. *Science* **2009**, *325*, 725−30.
(8) Wagenbauer, K. F.; Sigl, C.; Dietz, H. *Nature* **2017**, *552*, 78−83.
(9) Tikhomirov, G.; Petersen, P.; Qian, L. *Nature* **2017**, *552*, 67.
(10) Ong, L. L.; Hanikel, N.; Yaghi, O. K.; Grun, C.; Strauss, M. T.; Bron, P.; Lai-Kee-Him, J.; Schueder, F.; Wang, B.; Wang, P.; Kishi, J. Y.; Myhrvold, C.; Zhu, A.; Jungmann, R.; Bellot, G.; Ke, Y.; Yin, P. *Nature* **2017**, *552*, 72.
(11) Marras, A. E.; Zhou, L.; Su, H. J.; Castro, C. E. *Proc. Natl. Acad. Sci. U. S. A.* **2015**, *112*, 713−8.
(12) Zhang, D. Y.; Winfree, E. *J. Am. Chem. Soc.* **2009**, *131*, 17303−17314.
(13) Andersen, E. S.; Dong, M.; Nielsen, M. M.; Jahn, K.; Subramani, R.; Mamdouh, W.; Golas, M. M.; Sander, B.; Stark, H.; Oliveira, C. L.; Pedersen, J. S.; Birkedal, V.; Besenbacher, F.; Gothelf, K. V.; Kjems, J. *Nature* **2009**, *459*, 73−6.
(14) Simmel, F. C.; Yurke, B. *Appl. Phys. Lett.* **2002**, *80*, 883−885.
(15) Pan, J.; Li, F.; Cha, T. G.; Chen, H.; Choi, J. H. *Curr. Opin. Biotechnol.* **2015**, *34*, 56−64.
(16) Zhang, D. Y.; Seelig, G. *Nat. Chem.* **2011**, *3*, 103−13.
(17) Rajendran, A.; Endo, M.; Hidaka, K.; Sugiyama, H. *J. Am. Chem. Soc.* **2013**, *135*, 1117−23.
(18) Kuzyk, A.; Yang, Y.; Duan, X.; Stoll, S.; Govorov, A. O.; Sugiyama, H.; Endo, M.; Liu, N. *Nat. Commun.* **2016**, *7*, 10591.
(19) Gerling, T.; Wagenbauer, K. F.; Neuner, A. M.; Dietz, H. *Science* **2015**, *347*, 1446−52.
(20) Bruetzel, L. K.; Gerling, T.; Sedlak, S. M.; Walker, P. U.; Zheng, W.; Dietz, H.; Lipfert, J. *Nano Lett.* **2016**, *16*, 4871−9.
(21) Russell, R.; Zhuang, X.; Babcock, H. P.; Millett, I. S.; Doniach, S.; Chu, S.; Herschlag, D. *Proc. Natl. Acad. Sci. U. S. A.* **2002**, *99*, 155−60.




DOI: 10.1021/acs.nanolett.8b00592
*Nano Lett.* XXXX, XXX, XXX−XXX

(22) Chen, S. J.; Dill, K. A. *Proc. Natl. Acad. Sci. U. S. A.* **2000**, *97*, 646−51.
(23) Lipfert, J.; Doniach, S. *Annu. Rev. Biophys. Biomol. Struct.* **2007**, *36*, 307−27.
(24) Svergun, D. I.; Koch, M. H. J. *Rep. Prog. Phys.* **2003**, *66*, 1735.
(25) Pollack, L.; Doniach, S. Time-resolved X-ray scattering and RNA folding. In *Methods in Enzymology: Biophysical, Chemical, and Functional Probes of RNA Structure, Interactions and Folding: Part B*; Elsevier Inc., 2009; Vol. *469*, pp 253−268.
(26) Hura, G. L.; Menon, A. L.; Hammel, M.; Rambo, R. P.; Poole, F. L., II; Tsutakawa, S. E.; Jenney, F. E., Jr.; Classen, S.; Frankel, K. A.; Hopkins, R. C.; Yang, S. J.; Scott, J. W.; Dillard, B. D.; Adams, M. W.; Tainer, J. A. *Nat. Methods* **2009**, *6*, 606−12.
(27) Fischer, S.; Hartl, C.; Frank, K.; Rädler, J. O.; Liedl, T.; Nickel, B. *Nano Lett.* **2016**, *16*, 4282−4287.
(28) Panine, P.; Finet, S.; Weiss, T. M.; Narayanan, T. *Adv. Colloid Interface Sci.* **2006**, *127*, 9−18.
(29) Kilchherr, F.; Wachauf, C.; Pelz, B.; Rief, M.; Zacharias, M.; Dietz, H. *Science* **2016**, *353*, aaf5508.
(30) Song, J.; Gomes, G.-N.; Shi, T.; Gradinaru, C. C.; Chan, H. S. *Biophys. J.* **2017**, *113*, 1012−1024.
(31) Fuertes, G.; Banterle, N.; Ruff, K. M.; Chowdhury, A.; Mercadante, D.; Koehler, C.; Kachala, M.; Estrada Girona, G.; Milles, S.; Mishra, A.; Onck, P. R.; Grater, F.; Esteban-Martin, S.; Pappu, R. V.; Svergun, D. I.; Lemke, E. A. *Proc. Natl. Acad. Sci. U. S. A.* **2017**, *114*, E6342−e6351.
(32) Kugel, W.; Muschielok, A.; Michaelis, J. *ChemPhysChem* **2012**, *13*, 1013−22.
(33) Graceffa, R.; Nobrega, R. P.; Barrea, R. A.; Kathuria, S. V.; Chakravarthy, S.; Bilsel, O.; Irving, T. C. *J. Synchrotron Radiat.* **2013**, *20*, 820−5.



DOI: 10.1021/acs.nanolett.8b00592
*Nano Lett.* XXXX, XXX, XXX−XXX